Optical properties of semiconducting iron disilicide thin films

M. C. Bost and J. E. Mahan

Department of Electrical Engineering and Condensed Matter Sciences Laboratory, Colorado State University, Fort Collins, Colorado 80523

Iron disilicide thin films were prepared by furnace reaction of ion beam sputtered iron layers with single-crystal silicon wafers and with low-pressure chemical vapor deposition (LPCVD) polycrystalline silicon thin films. X-ray diffraction indicates the films are single-phase, orthorhombic, β-FeSi$_2$. Impurity levels are below the detection limit of Auger spectroscopy. Normal incidence spectral transmittance and reflectance data indicate a minimum, direct energy gap of 0.87 eV. The apparent thermal activation energy of the resistivity in the intrinsic regime is about half of this minimum optical gap. With such a direct band gap, the material may be suitable for the development of both light-sensitive and light-emitting thin-film devices within the silicon microelectronics technology.

INTRODUCTION

The prospects of fabricating narrow-band-gap, semiconducting transition metal silicides within the planar silicon technology are intriguing from both practical and fundamental viewpoints. One may envision the development of new optoelectronic devices, and find a fertile field of research leading to a better fundamental understanding of the silicides as a class of materials.

The semiconducting nature of several transition metal silicides has been established in past investigations of the transport properties of bulk samples. Table I gives previously published values of the forbidden energy gaps of the semiconducting phases thought to be of essentially stoichiometric composition. These values, the simplest interpretation of them being the 0 °K energy gaps, were inferred from the temperature dependence of the electrical resistivity or in some cases of the Hall coefficient. There are other apparently semiconducting phases whose compositions are less well defined. These include MnSi$_{1.7}$ [having reported band-gap values of 0.4,[9] 0.702,[10] and 0.9 eV,[7] and IrSi$_{1.75}$(1.2 eV)].[11]

There are a variety of ways in which the semiconducting nature of a substance may be revealed. The concept of the minimum metallic conductivity was introduced by Mott, who put an upper limit of about 3,000 $\mu\Omega$ cm on the resistivity of a metallic phase.[12] The semiconducting manganese silicide has been reported to exhibit a resistivity as high as 0.1 Ω cm,[13] and the iridium silicide was prepared in thin-film form having a room temperature resistivity of 6.7 Ω cm. The thermally activated character of the resistivity usually is a reliable indicator of the semiconducting state; it has been the basis for classifying almost all of the previously mentioned silicides as semiconductors. Perhaps the most direct indicator of semiconduction is the observation of an optical-absorption edge. The semiconducting nature of the iridium silicide was demonstrated in this way, the data being consistent with a direct transition.

The optical properties of most of the semiconducting silicides are unknown, because most property studies of these have been done on bulk samples which absorb very strongly above the fundamental edge. However, these materials may be prepared in thin-film form by codeposition of metal/silicon mixtures or by furnace reaction of the deposited metal film with a silicon substrate. Because of the obvious opportunity for developing, within the planar silicon technology, new optoelectronic devices that could operate in the infrared region, a fundamental investigation of the optical and photoelectronic properties seems long overdue. To that end, we have prepared FeSi$_2$ thin films and have investigated their optical properties, which are described below.

SAMPLE PREPARATION AND MATERIALS CHARACTERIZATION

Iron disilicide may assume two crystal structures: a low temperature, orthorhombic, semiconducting β phase, and a high temperature, tetragonal, metallic α phase. There is some uncertainty regarding the transition temperature. Values given are 915,[14,15] 937,[5] 950,[15] and 960 °C.[6] The composition range of the α phase is thought to be rather broad, extending from 69.6 to 72.1 at. % silicon (the excess silicon being due to vacancies in the iron sublattice). The β phase has not been found to deviate detectably from the stoichiometric composition, when carefully prepared.[16]

Thin films of iron disilicide were prepared by furnace reaction (in 99.995% pure argon) of ion beam sputtered iron

TABLE I. Semiconducting transition metal silicides.

Material	Forbidden energy gap	Reference
CrSi$_2$	0.35 eV	1
	0.30	2
FeSi$_2$	1.38	3
	0.9–1.0	4
	0.85	5
	0.7–0.8	6
	0.8	7
LaSi$_2$	0.19	7
ReSi$_2$	0.12	7
BaSi$_2$	0.48	7
OsSi$_2$	1.8	8
Ca$_2$Si	1.9	7
Mg$_2$Si	0.75	7

TABLE II. X-ray diffraction peaks used in phase identification.

Phase	Two theta	Miller indices
FeSi	28.2°	(110)
	34.6°	(111)
	45.3°	(210)[a]
	50.1°	(211)
β-FeSi$_2$	29.2°	(220) and (202)[a]
	46.0°	(313) and (331)
	46.6°	(040)
	49.5°	(422)
α-FeSi$_2$	17.4°	(001)[a]
	37.8°	(101)
	49.1°	(102)
	53.6°	(113)

[a] The most intense peak.

layers (99.99% purity sputtering target) with polished silicon wafers [n type, (100), 20–50 Ω cm], and with similar wafers that (before iron deposition) were thermally oxidized to 1000 Å and coated with 5000 Å of polycrystalline silicon (polysilicon) by low-pressure chemical vapor deposition. In the search for suitable furnace annealing conditions, FeSi as well as the two disilicide phases were observed. The furnace cool down, though requiring several hours, was sufficiently rapid to obtain the metastable α phase. It was found that a few prominent and unique x-ray diffraction peaks associated with each phase could be utilized for phase identification in the furnace-reacted films. The two-theta values of these peaks for copper K-α radiation, and their Miller indices, are given in Table II.[17]

For 1000 and 1050 °C anneals (all anneals were for 120 min except as specifically mentioned below), the only detectable phase formed on either substrate type was α-FeSi$_2$. For 850 and 900 °C, x-ray diffraction revealed β-FeSi$_2$, with one wafer out of twelve exhibiting a single prominent FeSi peak (a 30-min anneal at 900 °C yielded samples exhibiting several FeSi peaks and some from β-FeSi$_2$). It was found that at 950 °C a mixture of the α- and β-disilicide phases was obtained, with the β phase enhanced for the polysilicon-coated substrate as compared to the bare wafer. A "thick" iron layer (over 1500 Å) favored β-FeSi$_2$ formation, while a "thin"

layer (under 1000 Å) favored the α phase. Indeed, a radial variation in the relative amounts of the α and β phases over the 4-in.-diam silicon substrates corresponds in this way to the radial variation in the sputtered iron layer thickness. This is consistent with the previously reported tendency of the α phase to be deficient in iron.

An annealing temperature of 900 °C was selected to prepare β-FeSi$_2$ layers of the highest possible quality on single-crystal substrates for the optical measurements. A representative x-ray diffraction pattern is shown in Fig. 1 for a 6700-Å film. The peaks are labeled with the Miller indices of β-FeSi$_2$. A so-called "forbidden" silicon peak, due to multiple reflections in the single-crystal substrate, is also seen. Compositional analysis by Auger spectroscopy is given in Fig. 2. The Auger spectra, obtained after ion milling for several minutes into the film, exhibit strong Fe(LMM) and Si(KLL) peaks. The O(KLL) and C(KLL) signals, which were strong on the film surface, were below the detection limit of the intstrument within the interior of the films and are not seen in the data. The Ar(LMM) peak is an artifact due to the ion milling procedure; there were no other detectable impurities.

A scannning electron microscope (SEM) fracture cross section of a typical sample is shown in Fig. 3. Clearly visible are the β-FeSi$_2$ film and the underlying single-crystal silicon substrate. The film thickness is approximately 8000 Å; surface roughness appears to be negligible for the optical measurements to be discussed below.

OPTICAL PROPERTIES

Transmittance and reflectance spectra for a series of film thicknesses are shown in Fig. 4. The light was incident on the silicide layer. The transmittance data are referenced to an identical bare silicon substrate. With increasing film thickness, the transmission for energies above that of the absorption edge and the interference fringe spacing below the edge decrease, as expected. These data were used, together with the optical model given in the Appendix, to obtain by a damped Newton fitting procedure[18] the complex index of refraction ($\tilde{n}_2$) of the silicide layer in the region of the fundamental absorption edge:

$$\tilde{n}_2 = n_2 + ik_2. \tag{1}$$

n_2 and k_2 are the real and imaginary parts, respectively. The model includes reflections at the front surface of the film,
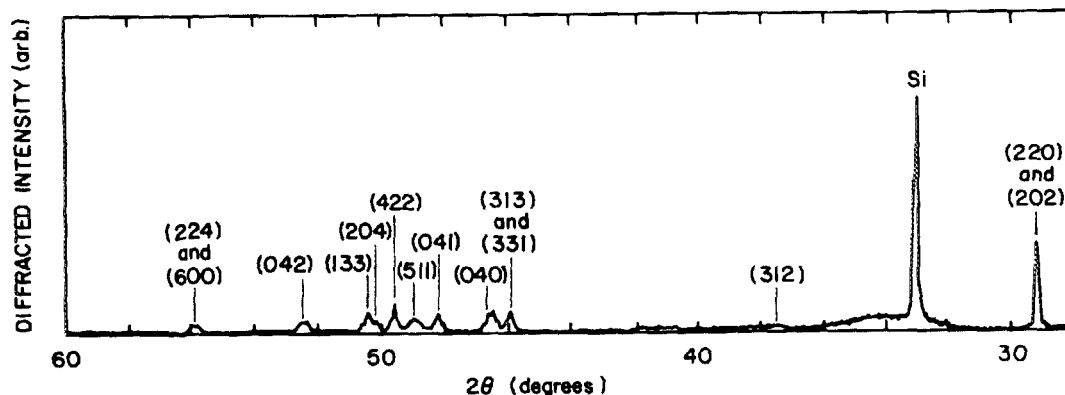

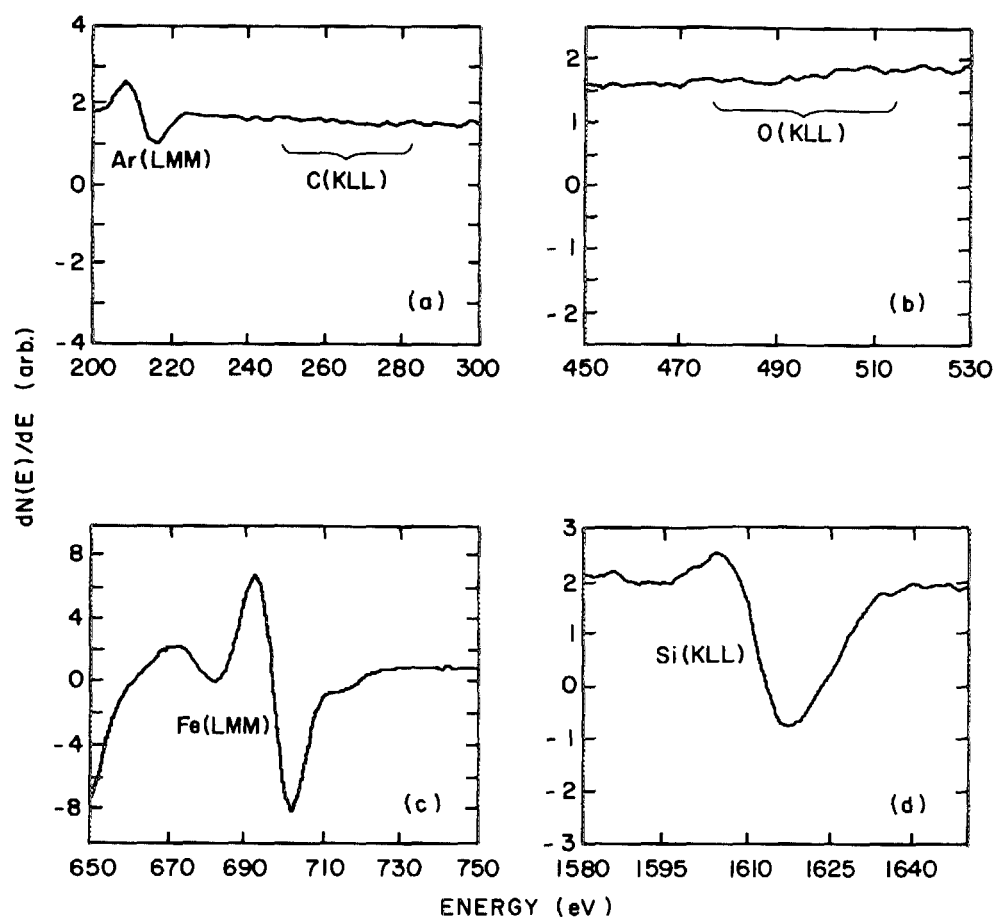FIG. 1. X-ray diffraction pattern for a β-FeSi$_2$ film prepared on a single-crystal substrate.

FIG. 2. Auger electron spectra in the appropriate energy windows for (a) argon and carbon, (b) oxygen, (c) iron, and (d) silicon, obtained after ion milling for several minutes into a β-FeSi$_2$ film.

multiple internal reflections in both the film and the substrate, and absorption within the silicide film but not in the substrate. Values for the index of refraction of the silicon substrate were obtained from Briggs.[19] The data were smoothed by averaging the value of a data point and each neighbor, with the center point being weighted twice as much as either neighbor.[20]

The optical-absorption coefficient (K_2), calculated from

$$K_2 = 4\pi k_2/\lambda \tag{2}$$

(λ being the wavelength) and the data of Fig. 4, is shown in Fig. 5. The onset of absorption just below 0.5 eV is due to extrinsic transitions involving defect states within the forbidden energy gap, while the second rise above 0.8 eV indicates the onset of the fundamental interband transitions. The data have been replotted in Fig. 6 in a manner that would yield a linear plot for direct allowed transitions, with the intercept indicating the minimum photon energy (E_g) required[21]:

$$(K_2 h\nu)^2 = C (h\nu - E_g). \tag{3}$$

h is Planck's constant, ν is the frequency, and C is a constant depending on the details of the band structure. It does appear that the transition is direct, with a value of 0.87 eV for the minimum photon energy.

The solid line in the figure was fitted to the data using the method of least squares. Data below 0.88 eV were not used for the fit. An analogous plot of $(K_2 h\nu)^{1/2}$ versus photon energy, which would be appropriate for an indirect gap,[21,22] is not linear over any appreciable energy range.

Our belief that the absorption below the fundamental edge is due to defects is consistent with the fact that the material is in the form of a fine-grained polycrystalline thin film. A similar absorption tail has been observed for grain boundary defect states in fine-grained polysilicon.[23] The defect part of the absorption coefficient was obtained by subtracting from the data the part due to interband transitions; the results are shown in Fig. 7 together with the fundamental edge as obtained from the fitting procedure of Fig. 6. The defect absorption spectrum indicates a peak in the density of states at 0.6 eV from either the valence- or the conduction-band edge. If the constant of proportionality were known, it would be possible to estimate the total defect state density from the magnitude of the absorption constant as has been done for amorphous silicon.[24] Alternatively, assuming an optical cross section of 10^{-15} cm^2 gives a density on the order of 10^{19} cm^{-3}. This cross section is typical of impurity levels in silicon materials used as extrinsic photoconductive detectors.[25]

Electrical measurements on the films formed on bare silicon wafers are not meaningful due to the shorting effect of the substrate, but conductivity data have been obtained for films made by an identical procedure on thermally oxidized and polysilicon-coated substrates as described above. The behavior of a representative sample is shown in Fig. 8. The temperature dependence indicates the films are extrinsic at room temperature, where the value is ~ 1 (Ω cm)$^{-1}$. Above ~ 500 K the conductivity is thermally activated with an apparent activation energy of ~ 0.43 eV. The simplest interpretation is that the material has become intrinsic with the acti-
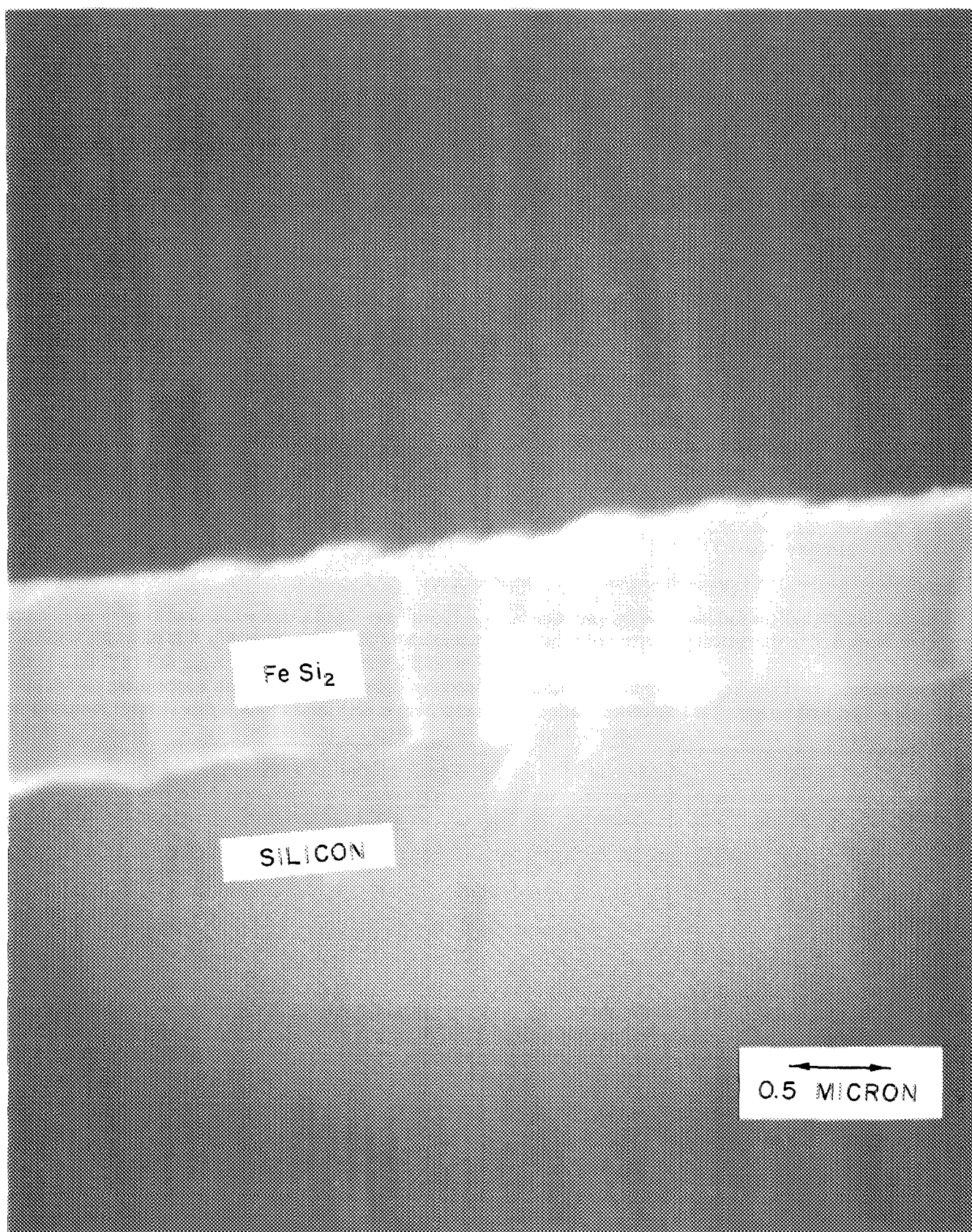
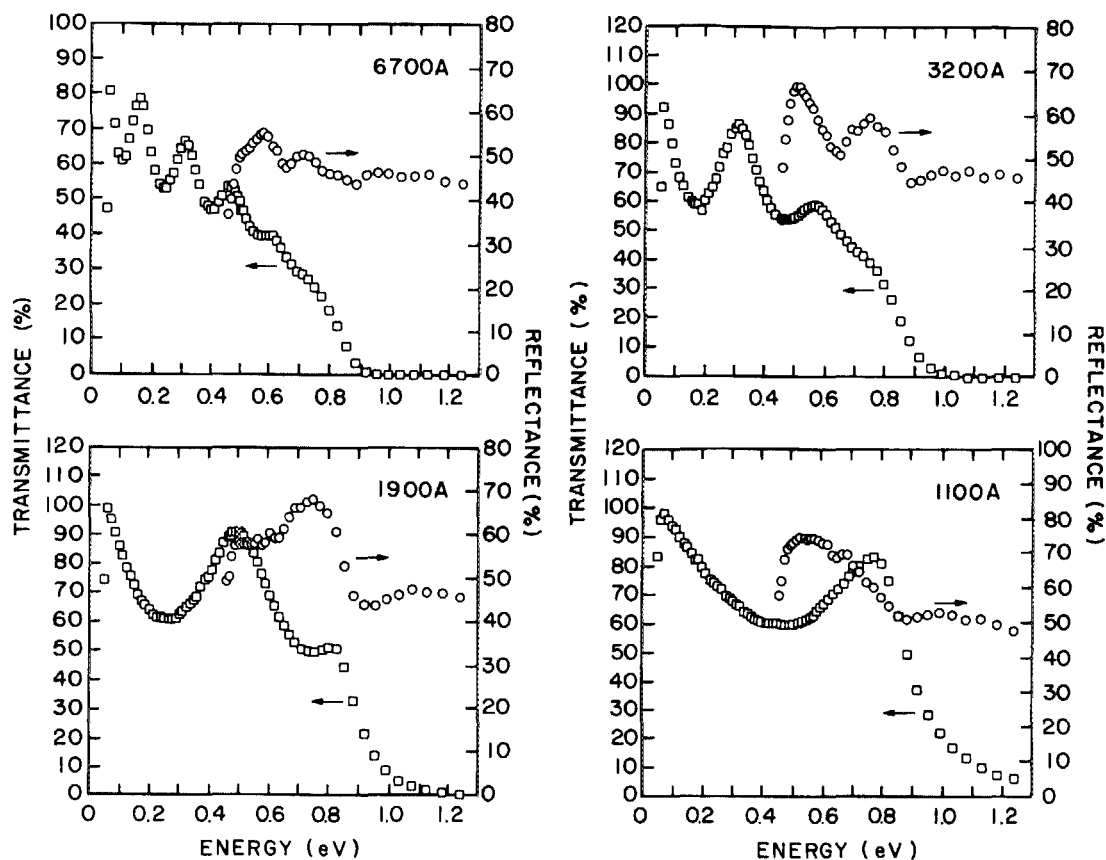FIG. 3. SEM fracture cross section showing β-FeSi$_2$ prepared on a bare silicon wafer.

FIG. 4. Spectral transmittance and reflectance data for films of four different thicknesses.

vation energy equal to half the forbidden energy gap, which corresponds fairly well to the optically determined value of 0.87 eV.

Room-temperature Hall-effect measurements indicated the films are p type, with an apparent hole concentration of $\sim 2 \times 10^{18}$ cm^{-3} and a Hall mobility of 3 cm^2/V s. At room temperature the resistivity in Fig. 8 is thermally activated but with a smaller activation energy (0.13 eV) than in the intrinsic regime. Thus, the room temperature carrier concentration is determined by acceptor states separated from
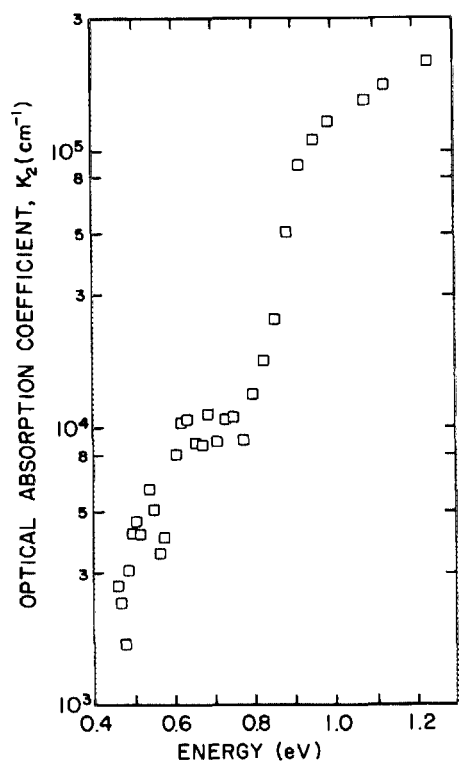
FIG. 5. Optical-absorption coefficient vs photon energy.
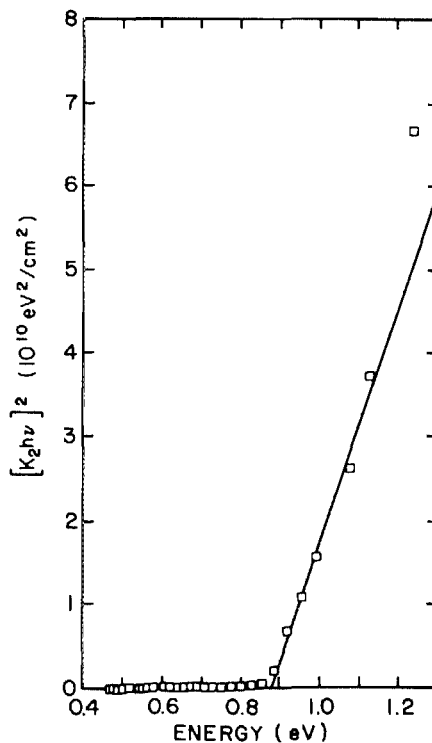
FIG. 6. Absorption coefficient data showing the existence of a direct transition.
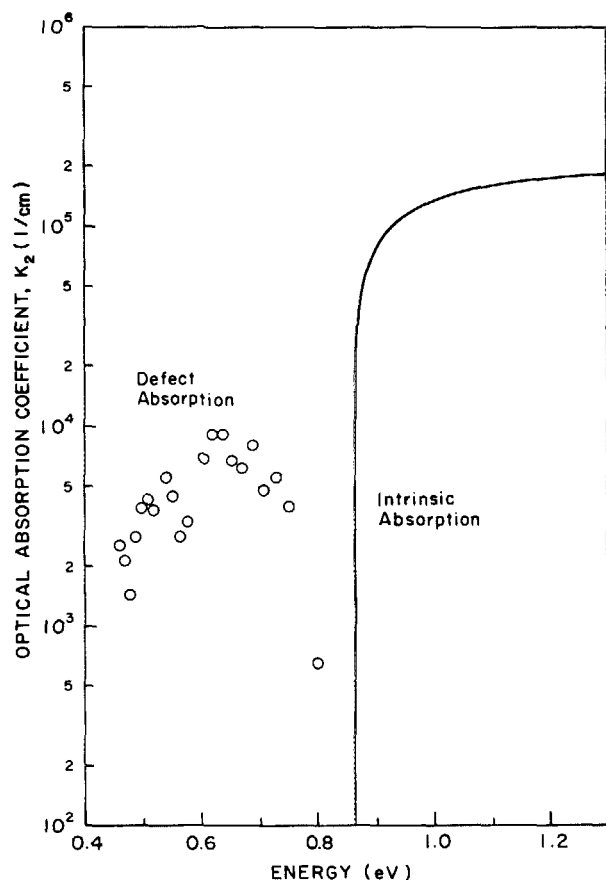
FIG. 7. Defect part of the optical-absorption coefficient.
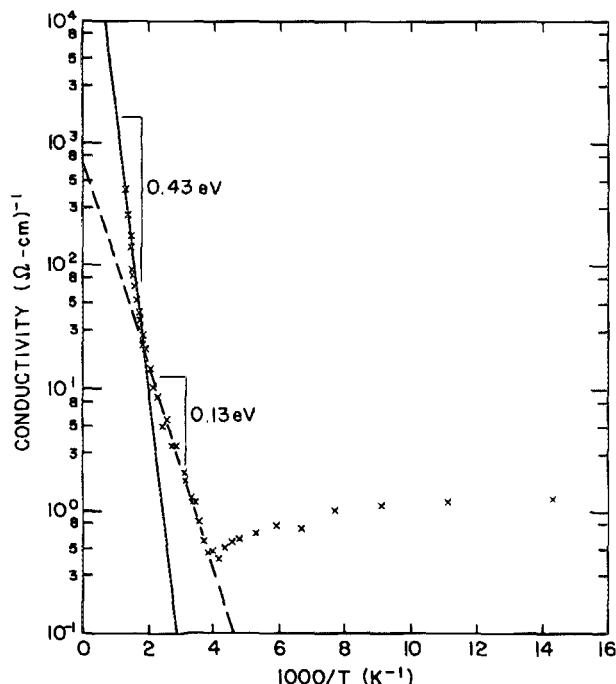

FIG. 8. Electrical resistivity vs temperature; the solid line corresponds to a thermal activation energy of 0.43 eV and the dashed line, to 0.13 eV.

the valence-band edge by this energy (making the reasonable assumption that they are partially compensated). Thermo-electric probing of the films formed on polysilicon also indicated p-type conduction. In previous publications the transport properties of β-FeSi₂, when prepared as an n-type material, have been modeled extensively with the small polaron model[4,26]; when not intentionally doped, it was found generally to be p type and a free-hole band model was used.

Finally, in Fig. 9 we show the real and imaginary parts of the complex index of refraction and for comparison, the real (e_{21}) and imaginary (e_{22}) parts of the complex relative permittivity $(\bar{e}_2)$, calculated from

$$e_{21} = (n_2)^2 - (k_2)^2 \qquad (4)$$

and

$$e_{22} = 2n_2 k_2. \qquad (5)$$

The values for k_2 and e_{22} are fairly typical, as may be seen by examining several recent reviews of the optical properties of semiconductors,[21,27,28] but data on the spectral variation of the real parts of $\tilde{n}_1$ and $\tilde{e}$ in the vicinity of the absorption edge is surprisingly scarce. n_1 and e_1 for germanium and silicon peak slightly *above* the absorption edge (instead of below it as our values for FeSi₂ do), with maximum values for e_1 of ~30 and ~45, respectively.[28,29] InSb exhibits a maximum value for e_1 of ~25 just above its band edge.[30] Lead salt semiconductor materials have high-frequency relative permittivities (optically determined) on the order of 200–400.[31]

The data representing $\tilde{n}$ and $\tilde{e}$ in the energy range of defect absorption is not necessarily the material's intrinsic behavior. The same defect states that give the prominent extrinsic absorption below the fundamental edge produce additional structure in the imaginary parts of $\tilde{n}$ and $\tilde{e}$ in this energy range and may also increase the optical dielectric constant (e_1) there.[32]

There have been some previous investigations of the optical properties of β-FeSi₂ by Bircholz and co-workers, primarily concerned with the spectral region of lattice and impurity absorption.[26,33] The modulus of the relative dielectric constant $[(n_2)^2 + (k_2)^2]$ was found to attain values of several hundred in the range of lattice vibrations (20–40 μm). A limiting high-frequency value of 27.6 was observed, which is consistent with our data in this range. The spectral range near their absorption edge (1.3 μm or equivalently 0.95 eV, as was reported) was not studied in detail, but it was indicated that n increases with decreasing energy below E_g. To our knowledge, this is the extent of the previous literature on the optical properties of β-FeSi₂ in the vicinity of the absorption edge.

SUMMARY AND CONCLUSIONS

Semiconducting β-FeSi₂ thin films exhibit a minimum direct forbidden energy gap of 0.87 eV. With such a direct gap the material may be suitable for the development of both light-sensitive and light-emitting devices that may be fabricated within the silicon microelectronic technology.
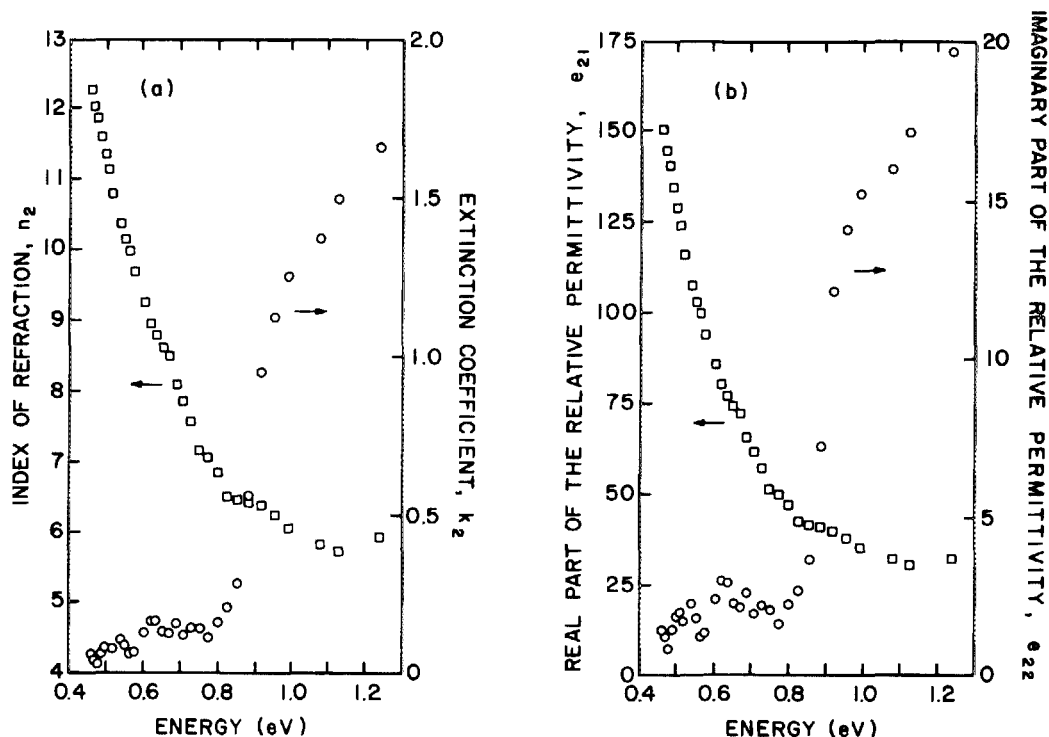
FIG. 9. Real and imaginary parts of (a) the complex index of refraction, and (b) the relative permittivity.

ACKNOWLEDGMENTS

APPENDIX: DERIVATION OF THE NORMAL INCIDENCE TRANSMITTANCE AND REFLECTANCE OF A THIN-FILM-SUBSTRATE SYSTEM

In this Appendix, expressions for the normal incidence transmittance and reflectance of a two-layer system are derived. To model the data correctly, it is necessary to consider absorption in the thin film and to include multiple internal reflections in both the thin film and the substrate. Several pioneering optical papers[34,35] and standard optical reference works[36-38] provide expressions for the reflectance and transmittance of a two-layer system, but none provide derivations based on all of the above assumptions.

The radiation is incident on an absorbing layer, and the transmitted part exits through a relatively thick, nonabsorbing substrate as shown in Fig. 10. It is assumed that the imaginary parts of the indices of refraction of both the substrate (medium III and the air (medium I) are negligible.

The transmission phasor for medium II is given by the well-documented formula[34-38]:

$$t_{\mathrm{II}} = \frac{t_{12}t_{23} \exp[i(Z_2) - K_2d_2/2]}{1 - r_{23}r_{21} \exp[i(2Z_2) - K_2d_2]}. \quad (A1)$$

Similarly, the reflection phasors for light entering medium two from either the front (r_{IIF}) or the back (r_{IIB}) are[36,38]

$$r_{\mathrm{IIF}} = \frac{r_{12} + r_{23} \exp[i(2Z_2) - K_2d_2]}{1 - r_{23}r_{21} \exp[i(2Z_2) - K_2d_2]} \quad (A2)$$

and

$$r_{\mathrm{IIB}} = r_{32} + \frac{t_{32}t_{23}r_{21} \exp[i(2Z_2) - K_2d_2]}{1 - r_{21}r_{23} \exp[i(2Z_2) - K_2d_2]}, \quad (A3)$$

where t_{ij} and r_{ij} are the Fresnel coefficients of the various interfaces, with the light traveling from medium i into medi-
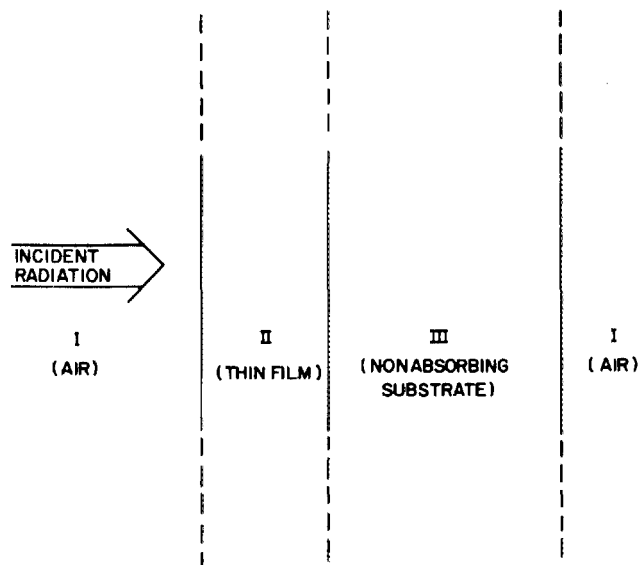

FIG. 10. Schematic diagram of the two-layer optical model.

um j. d_i is the thickness of medium i and Z_i is the phase thickness in vacuum wavelengths.

Medium II and its two interfaces may now be represented mathematically as a single interface on medium III with effective Fresnel coefficients t_{II}, r_{IIF}, and r_{IIB}.[36] The trans-

mission phasor for the full two-layer system is then

$$t = \frac{t_{II}t_{31}\exp(-iZ_3)}{1 - r_{IIB}r_{31}\exp[i(2Z_3)]} \tag{A4}$$

and the full reflection phasor is

$$r = \frac{r_{II} + r_{II}r_{12}r_{23}\exp[i(2Z_2) - K_2d_2] + r_{31}r_{12}r_{23}\exp[i(2Z_3)] + r_{31}\exp[i(2Z_3 + 2Z_2) - K_2d_2]}{1 + r_{13}r_{IIB}\exp[i(2Z_3)] + r_{12}r_{23}\exp[i(2Z_2) - K_2d_2] + r_{12}r_{13}r_{23}r_{IIB}\exp[i(2Z_3 + 2Z_2) - K_2d_2]}. \tag{A5}$$

The transmission phasor of a bare substrate is

$$t_s = \frac{t_{13}t_{31}\exp(iZ_3)}{1 - r_{13}r_{31}\exp(i2Z_3)}. \tag{A6}$$

Using Eqs. (A4)–(A6) and the standard definitions for the phase thickness of a layer and the Fresnel coefficients of an interface,[36] the reflectance and transmittance (referenced to that of a bare substrate) of the two-layer system may be calculated from

$$R = rr^* \tag{A7}$$

and

$$T = \frac{tt^*}{t_st_s^*}. \tag{A8}$$

[1]D. Shinoda, S. Asanabe, and Y. Sasaki, J. Phys. Soc. Jpn. **19**, 269 (1964).

[2]I. Nishida and T. Sakata, J. Phys. Chem. Solids **39**, 499 (1978).

[3]R. M. Ware and D. J. McNeill, Proc. IEE **111**, 178 (1964).

[4]U. Birkholz and J. Schelm, Phys. Status Solidi **27**, 413 (1968).

[5]U. Birkholz and J. Schelm, Phys. Status Solid **34**, K177 (1969); U. Birkholz and A. Fruehauf, ibid. K181 (1969).

[6]H. P. Geserich, S. K. Sharma, and W. A. Theiner, Philos. Mag. **27**, 1001 (1973).

[7]G. V. Samsonov, No. 2 Properties Index (Plenum, New York, 1964), p. 161.

[8]K. N. Mason, Prog. Cryst. Growth Character. **2**, 269 (1979).

[9]I. Nishida, J. Mater. Sci. **7**, 435 (1972).

[10]I. Kawasumi, M. Sakata, I. Nishida, and K. Masumoto, J. Mater. Sci. **16**, 355 (1981).

[11]S. Petersson, J. A. Reimer, M. H. Brodsky, D. R. Campbell, F. d'Heurle, B. Karlsson, and P. A. Tove, J. Appl. Phys. **53**, 3342 (1982).

[12]N. F. Mott and E. A. Davis, Electronic Processes in Non-Crystalline Materials (Clarendon, Oxford, 1971), p. 26.

[13]M. Eizenberg and K. N. Tu, J. Appl. Phys. **53**, 6885 (1982).

[14]F. A. Sidorenko, P. V. Gel'd, and L. B. Dubrovskaya, Fiz. Met. Metalloved. **8**, 735 (1959).

[15]I. N. Strukov and P. V. Gel'd, Fiz. Met. Metalloved. **4**, 190 (1957).

[16]F. A. Sidorenko, P. M. Gel'd, and L. B. Dubrovskaya, Fiz. Met. Metalloved. **8**, 465 (1959).

[17]Powder Diffraction Data File, Card 1-1271 (American Society for Testing Materials, Philadelphia, PA); ibid., Card 1-1285; P. Y. Dusausoy, J. Protas, R. Wandji, and B. Roques, Acta Cryst. B **27**, 1209 (1971).

[18]M. J. D. Powell, "Minimization of Functions of Several Variables," in Numerical Analysis, an Introduction, edited by J. Walsh (Thompson, Washington, DC, 1967), p. 145.

[19]H. B. Briggs, Phys. Rev. **17**, 287 (1950).

[20]P. R. Bevington, Data Reduction and Error Analysis for the Physical Sciences (McGraw–Hill, New York, 1969), p. 255.

[21]T. S. Moss, G. J. Burrell, and B. Ellis, Semiconductor Opto-Electronics (Butterworth, London, 1973), p. 71.

[22]G. G. Macfarlane, T. P. McLean, J. E. Quarrington, and V. Roberts, Phys. Rev. **111**, 1245 (1958).

[23]W. B. Jackson, N. M. Johnson, and D. K. Beigelson, Appl. Phys. Lett. **43**, 195 (1983).

[24]W. B. Jackson and N. M. Amer, Phys. Rev. B **25**, 5559 (1982).

[25]D. Long, "Photovoltaic and Photoconductive Infrared Detectors," in Optical and Infrared Detectors, edited by R. J. Keyes (Springer, Berlin, 1977), p. 144.

[26]U. Birkholz and J. Naegele, Phys. Status Solidi **39**, 197 (1970).

[27]M. Balkanski, in Vol. 2 of Handbook on Semiconductors, edited by T. S. Moss (North–Holland, Amsterdam, 1980).

[28]G. Harbeke, "Optical Properties of Semiconductors," in Optical Properties of Solids, edited by F. Abeles (North–Holland, Amsterdam, 1972), Chap. 2.

[29]F. Wooten, Optical Properties of Solids (Academic, New York, 1972), Chap. 3.

[30]H. Y. Fan, "Photon-Electron Interaction, Crystals without Fields," in Encyclopedia of Physics, Vol. XXV/2a, edited by S. Flugge (Springer, Berlin, 1967), p. 206.

[31]J. T. Longo, D. T. Cheung, A. M. Andrews, C. C. Wang, and J. M. Tracy, IEEE Trans. Electron Devices ED-25, 213 (1978).

[32]U. Birkholz, H. Finkenrath, J. Naegele, and N. Uhle, Phys. Status Solidi **30**, K81 (1968).

[33]S. J. Fonash, "Dielectric Properties of Thin Films: Polarization and Effective Polarization," in Physics of Nonmetallic Thin Films, edited by C. H. S. Dupuy and A. Cachard (Plenum, New York, 1976), p. 225.

[34]W. H. Brattain and H. B. Briggs, Phys. Rev. **75**, 1705 (1949).

[35]J. F. Hall and W. F. C. Ferguson, J. Opt. Soc. Am. **45**, 714 (1955).

[36]O. S. Heavens, Optical Properties of Thin Solid Films (Academic, New York, 1955), Chap. 4.

[37]H. Anders, Thin Films in Optics (Focal, London, 1965), Secs. 1.2 and 1.3.

[38]M. Born and E. Wolf, Principles of Optics, Third Rev. Ed. (Pergamon, Oxford, 1965), Sec. 13.4.